A comparison of TLS-based and ALS-based techniques for Concrete Floor Waviness Assessment

N. Puri[a] and Y. Turkan[b]

[a]PhD Student, School of Civil and Construction Engineering, Oregon State University, Corvallis, OR 97331
[b]Assistant Professor, School of Civil and Construction Engineering, Oregon State University, Corvallis, OR 97331
E-mail: purin@oregonstate.edu, yelda.turkan@oregonstate.edu

Abstract –

Laser scanning-based techniques have been applied for checking the dimensional tolerances of concrete elements. Several studies utilized Terrestrial Laser Scanning (TLS) for measuring concrete floor waviness. The results of those efforts have shown that accurate floor waviness information can be obtained using TLS. Unmanned Aerial Vehicles (UAVs) mounted with cameras and 3D laser scanning sensors, referred to as Airborne Laser Scanning (ALS) hereafter, have versatile applications in construction, such as surveying, progress control, 3D modelling and inspections. As-built data collection for dimensional quality assessment can be a potential application of such technology. In particular, the application of ALS for assessing the waviness of concrete slabs warrants further exploration. This study presents the results of a comparative analysis of floor waviness measurement results obtained using ALS and TLS-based technologies. Continuous Wavelet Transform (CWT) is applied to the depth map derived from both point cloud datasets to obtain waviness information. Comparable results are obtained for the CWT scales of 30, 60 and 75. Detailed discussions on how the results can be improved are presented. The analysis of the accuracy of results obtained using ALS advances its application in the field of dimensional quality assessment.

Keywords –

TLS, ALS, Continuous wavelet transform, Depth map, Point cloud, Dimensional quality control, tolerance compliance

1 Introduction

The geometric dimensions of as-built concrete elements often fail to comply with the tolerances specified in the as-designed plans [1]. The factors that contribute toward such discrepancies include lack of attention to details included in the project specifications, low accuracy and precision issues that occur during the construction of elements, and the misinterpretation of information provided in the project specifications. Consequently, increasing tolerance accumulation may affect the aesthetics of concrete elements, affects the correct placement of adjacent concrete elements and negatively affects the structural health of components in severe cases [2]. Construction quality control inspectors collect data related to the quality of on-going construction for effectively designing solutions to correct any defects or discrepancies that are present on concrete surfaces. Thus, dimensional quality assessment ensures that constructed elements accurately reflect the dimensions and locations specified in the contract documents. For concrete floors, this is one of the most significant processes constituting the overall construction process. For instance, constructed floors that do not meet appropriate flatness and waviness requirements negatively affect the operation of Very Narrow Aisle (VNA) trucks in warehouses. Furthermore, the undesired waviness present on the floor surface can affect the racking height of such vehicles, and consequently, the static lean which ultimately may cause these vehicles roll over [3–5].

Existing methods commonly used in the industry such as the Straightedge Method, the F-number method (ASTM E1155)[6] and the Waviness Index (WI) method (ASTM 1486) share the common drawback as they yield sparse as-built measurements. In addition, the data collection process is time and labor intensive, given that the floor surface area in warehouse construction projects easily exceed 4,000 m^2 [3–5]. The method proposed in [3] utilizes a framework that uses lidar-based point clouds and the Continuous Wavelet Transform (CWT) to overcome these disadvantages and provides a novel framework for measuring floor waviness. This framework was further developed to process 2D as built information in the form of depth maps, as opposed to 1D survey lines derived from TLS-based point clouds to impart waviness information of newly constructed concrete slabs. This study focuses on performing a comparative analysis of the floor waviness

results obtained using point cloud data collected with a TLS and a lidar sensor mounted UAV. The method of comparison presented in this study uses waviness detection results from TLS point clouds as ground truths, and relies on recall and precision rates to determine the accuracy of waviness results obtained using ALS point clouds.

2 Related Work

Lidar technology has a wide range of applications in the civil engineering industry, such as quantifying erosion rates and surface deformation [7], to landslide inventorying and assessing hazards [8], structural health monitoring [9–12], road roughness quantification [13–17] and survey and maintenance of historic buildings [18–20]. In the construction industry, lidar is primarily used for as-built documentation that supports progress tracking [3]–[7], facility management [8]–[13], dimensional quality control [3–5,32–34] in construction projects. In the area of dimensional quality control, lidar technology is commonly used for acquiring as-built data, owing to its ability to capture millions of points with mm-level accuracy. The acquired data is processed with the help of a multitude of algorithms, based on the desired applications. Few of the applications include assessing the flatness of the exterior facades using a color map derived from TLS point clouds [35], visualizing the elevation differences across a floor using elevation map generated from point cloud data [36] and assessing the dimensional compliance of concrete elements using BIM and TLS-based point cloud data [37]. Lidar-based point clouds, with the application of the Continuous Wavelet Transform (CWT), were also used in the assessment of floor waviness in [3,4]. The study in [3] demonstrated the efficacy of applying the two-dimensional CWT (2D CWT) to lidar-based point cloud data for assessing the waviness of concrete surfaces. The comparative analysis between results obtained using the framework and those obtained using the Waviness Index (WI) method showed that the framework accurately identifies regions on the floor where surface waviness of different characteristics exist. The framework utilized TLS-derived point cloud data for assessing the surface waviness of concrete floors.

Unmanned Aircraft Systems (UAVs) are exponentially gaining popularity for collecting as-built data from construction sites. UAVs mounted with photographic cameras, thermal cameras and lidar sensors or “pucks” have been widely used for survey data collection. Compared to TLS, UAV-mounted lidar sensors are capable of collecting data from large survey areas in a non-intrusive manner with limited occlusions [38,39]. For instance, a person standing in front of the laser scanner can create a larger obstruction during data collection using TLS, compared to ALS. Moreover, using TLS for collecting as-built data from working surfaces may hinder on-going operations and may interrupt workers on the surface. Thus, the objective of this paper is to compare the results of floor waviness obtained using point clouds derived from TLS and ALS. The framework proposed in [3,5] will be used for obtaining surface waviness results.

3 Analysis

3.1 Data Collection and Preprocessing

The data was collected from a newly constructed floor of a lecture hall under the Magruder Hall Expansion project in Corvallis, OR. Figure 1. shows the region of interest, and its surface area was approximately 140 m2. The Leica P40 scanner was setup in two locations across the floor. After registering the two scans, the spatial resolution of the output point cloud was approximately 5 mm within a range of 10 m. The Riegl miniVUX was used for obtaining the ALS point cloud. The UAV mounted with the lidar sensor was flown at a constant height of approximately 60 m above the surface of the ground, making two passes over the area of interest. It is assumed that the beam divergence is constant throughout the flight. The spatial resolution of the output point cloud collected from the UAV system was approximately 5 cm.

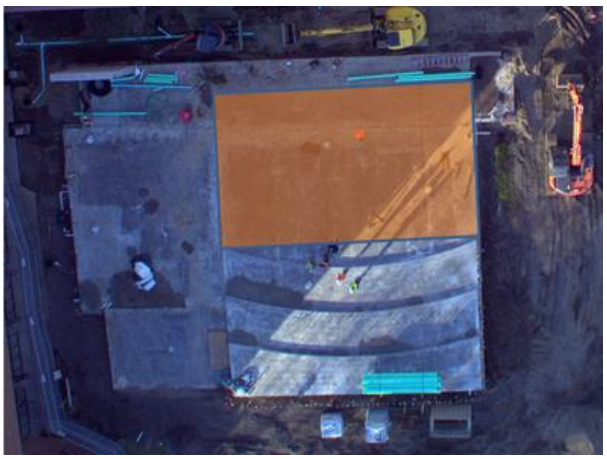

Figure 1. The region of interest is marked in orange.

3.2 Data Processing

The framework developed in [3] was used to process the data obtained from TLS and ALS. The obtained point clouds from the TLS and ALS systems were imported into a commercial point cloud processing software to remove scans corresponding to workers

working on the floor and various construction debris. A depth map is developed using triangulation-based linear interpolation on a grid with regular intervals of 1 cm. This process generated a map showing z-coordinates at each query point, where each query point is represented by the intersection of lines on the x-y plane of the grid. CWT, using the Mexican Hat wavelet as the mother wavelet, was applied to the depth map at different scales. To simplify the analysis, only five scales were chosen for the CWT: 15, 30, 45, 60 and 75. The five scales correspond to the five undulation periods in the WI method: 2, 4, 6, 8 and 10 ft, respectively. The correspondence between the WI index values and the CWT scales are shown in Table 1.

Table 1**.** Waviness Index values and corresponding continuous wavelet transform scales [3][4]

Characteristic period (T) [cm]	CWT scale (a)	Waviness Index (k values)
61	15	1
121.9	30	2
182.9	45	3
243.8	60	4
304.8	75	5

3.3 CWT Results

The surface waviness results obtained for the TLS- and ALS-based point clouds, for scales 15, 30, 45, 60 and 75, are shown in Figure 2, Figure 3, Figure 4, Figure 5 and Figure **6**, respectively. The peaks detected for the CWT responses for these five scales are presented.

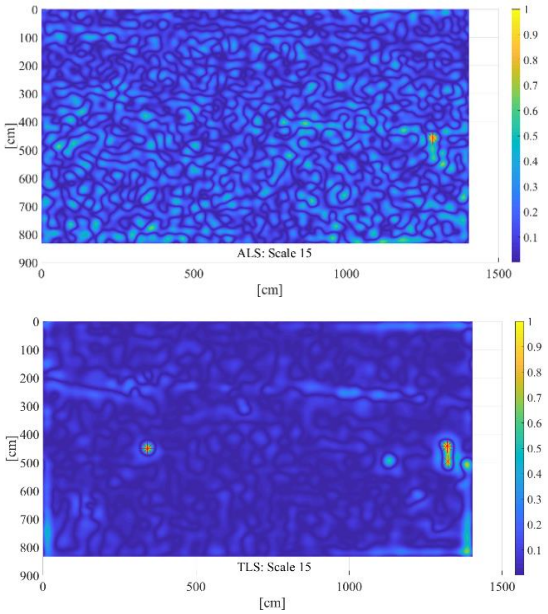

Figure 2. The results of the CWT analysis at scale 15 with peak detection (red asterisk) for the ALS (top) and TLS point clouds (bottom)

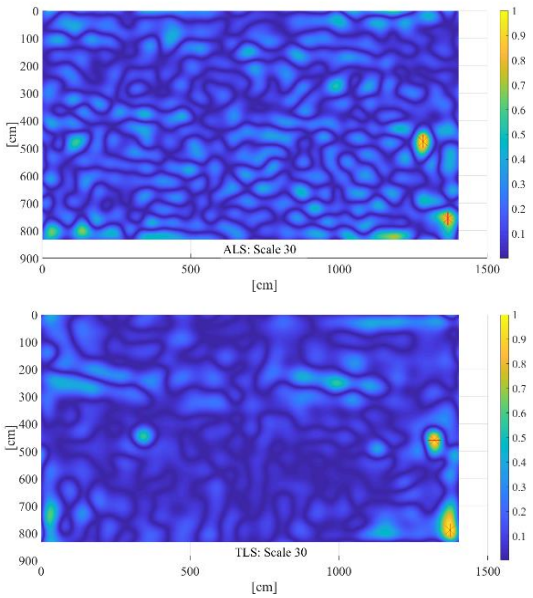

Figure 3. The results of the CWT analysis at scale 30 with peak detection (red asterisk) for the ALS (top) and TLS point clouds (bottom)

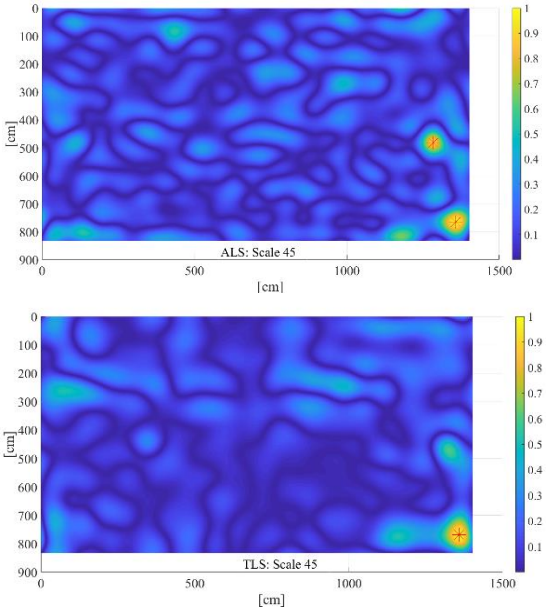

Figure 4. The results of the CWT analysis at scale 45 with peak detection (red asterisk) for the ALS (top) and TLS point clouds (bottom)

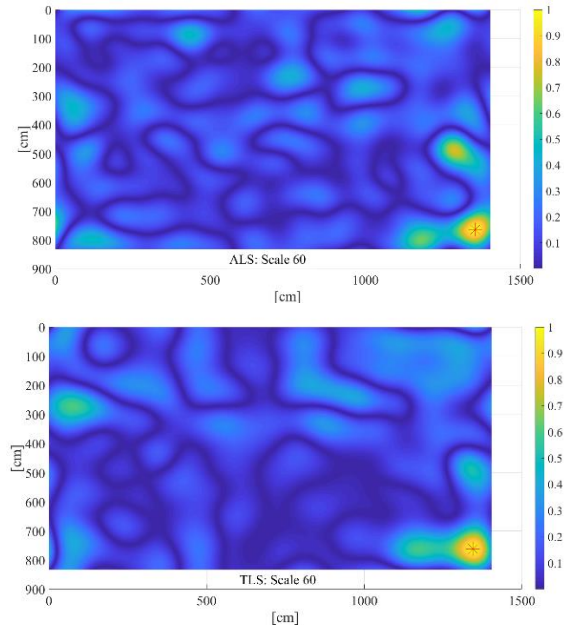

Figure 5. The results of the CWT analysis at scale 60 with peak detection (red asterisk) for the ALS (top) and TLS point clouds (bottom)

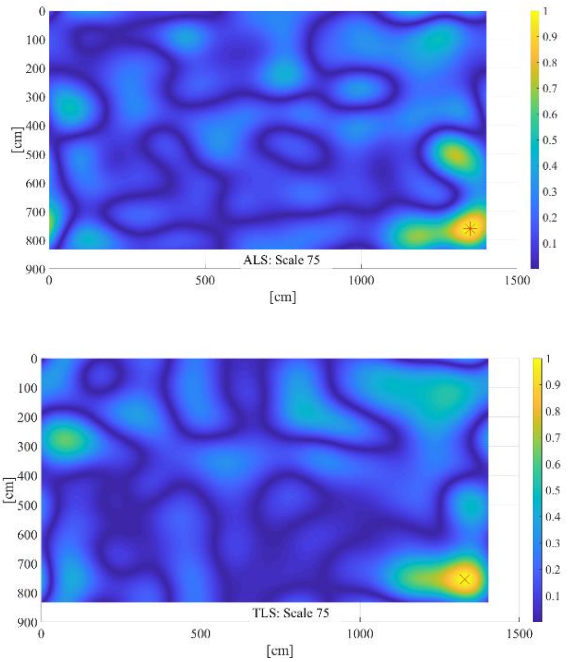

Figure 6. The results of the CWT analysis at scale 75 with peak detection (red asterisk) for the ALS (top) and TLS point clouds (bottom)

As shown in Figure 2, Figure 3, Figure 4,Figure 5, and Figure **6**, peak responses for the CWT coefficient values lie 10% below the maximum value. The location of these peak responses for each of the five scales are used for our analysis.

The waviness results obtained from the TLS-based point clouds are used as ground truth for measuring the performance of the ALS-based point clouds for generating the waviness results. The convention of true positives (TP), true negatives (TN), false positives (FP) and false negatives (FN) that applies to the peak detection problem in our study is shown in Table 2. The number of true positives, true negatives, false positives and false negatives are shown in Table 3.

Table 2. Convention of the true positive, true negative, false positive and false negative for peak detection

	Peak present (TLS)	**Peak absent (TLS)**
Peak detected (ALS)	TP	FP
Peak not detected (ALS)	FN	TN

Table 3. Total number of true positives (TP), true negatives (TN), false positives (FP) and false negatives (FN)

Scales	**TP**	**TN**	**FP**	**FN**	**Actual number of peaks (TLS based)**
15	1	0	0	2	3
30	2	0	0	0	2
45	1	0	1	0	1
60	1	0	0	0	1
75	1	0	0	0	1

In the TLS based results, for scale 15, the ground truth shows that there are 3 peaks that correspond to undulations having a characteristic period of 61 cm. Only one of those peaks are detected in the waviness results derived from the ALS point cloud. For scale 30, two peaks that correspond to the characteristic period of 121.9 cm were detected in both the TLS and ALS based results. At scale 45, one peak corresponding to 182.9 cm was obtained in the TLS and two peaks in the ALS based results. Similarly, for scales 60 and 75, 1 peak corresponding to the characteristic period of 304.8 cm was detected in both the TLS and ALS based results. Table 4 shows the correspondence between the waviness detection results obtained using TLS and ALS using precision and recall rates for the five scales selected in this study.

Table 4**.** Recall, precision and accuracy rates

Scales	**15**	**30**	**45**	**60**	**75**
Recall	33%	100%	100%	100%	100%
Precision	100%	100%	50%	100%	100%

Accuracy	33%	100%	100%	100%	100%
F-Score	0.5	1	0.67	1	1

The surface waviness results for scales 60 and 75 using the TLS and ALS based point clouds are comparable. For scale 45, a false positive was detected near [1283 cm, 481 cm]. The same region near the TLS was inspected and no peak was found. The CWT response at that region for the ALS based results was 0.8816, and 0.1674 for the TLS. This discrepancy might be attributed to the difference in the z-values shown in the depth maps of the TLS and ALS point clouds. The TLS based depth map shows the elevation at [1283 cm, 481 cm] to be approximately 2.8 cm and the ALS based depth map shows 1.75 cm. Although the TLS and ALS scans were collected almost simultaneously, there were workers actively working on the work surface. This may be due to dynamic changes resulting from moving objects or debris on the floor surface. Another reason may be due to the low resolution of the ALS point cloud. For scale 15, the results are not comparable to each other. A possible reason could be that using TLS-based high-resolution point cloud helped detect undulations of a lower characteristic period (61 cm) accurately. The lower resolution ALS-based point cloud may have failed to capture those undulations. While generating the depth map, the z-coordinates are smoothed out to a higher degree if there were fewer neighbouring points present around the query points.

4 Discussions and Conclusions

The efficacy of using ALS-derived point clouds for detecting surface waviness of concrete floors was examined. Using the UAV mounted with lidar can help quality control inspectors to non-intrusively collect as-built point cloud from concrete slabs. The analysis of the CWT results show that the surface waviness detection results are not comparable for scales 15 and 45. The analysis showed comparable results for detecting the undulations corresponding to scales of 30, 60 and 75. In summary, one of the possible reasons for discrepancies in the two results is the difference in the resolution of both point clouds. The resolution of the TLS based point cloud was approximately 10 times better than that of the ALS based point cloud. The other reason could be due to the misalignment of both point clouds. The targets placed on the ground were visible in the TLS data, but were not clearly visible in the ALS point clouds. Two solutions are proposed: 1) Flying the UAV closer to the ground: The lower the aircraft flies, the smaller the lidar footprint diameter will be, which results in a higher density of points per scanning area. Decreasing the lidar footprint is essential for detecting small changes in elevation across the surfaces. A good option would be flying under 15 m. 2) Increase the number of passes: An increase in the number of passes will improve the resolution quality of the point cloud.

Future work will focus on examining the number of passes required to obtain a point cloud resolution that is comparable to that obtained using a TLS. In addition, the impact of the altitude difference for obtaining the desired resolution and capturing the small changes in elevation across the floor will be examined. Furthermore, the differences in the z-coordinates of the depth map resulting from the application of other interpolation methods will be evaluated.

5 Acknowledgements

The authors would like to thank Chase Simpson from Oregon State University and Jake Dafni from the NHERI RAPID Experimental Facility at the University of Washington for their help in collecting the data using the UAV and for preprocessing the data. The authors would also like to thank John M. Doty, the project manager, Scott Cach and the Fortis team for their help and cooperation throughout the data collection process.

6 References

[1] D.K. Ballast, Handbook of Construction Tolerances, Second, John Wiley & Sons, 2007.

[2] N. Puri, Y. Turkan, Toward Automated Dimensional Quality Control of Precast Concrete Elements Using Design BIM, WIT Transactions on The Built Environment. 169 (2017) 203–210.

[3] N. Puri, E. Valero, Y. Turkan, F. Bosché, Assessment of compliance of dimensional tolerances in concrete slabs using TLS data and the 2D continuous wavelet transform, Automation in Construction. 94 (2018) 62–72. doi:10.1016/j.autcon.2018.06.004.

[4] F. Bosché, B. Biotteau, Terrestrial laser scanning and continuous wavelet transform for controlling surface flatness in construction – A first investigation, Advanced Engineering Informatics. 29 (2015) 591–601. doi:10.1016/j.aei.2015.05.002.

[5] E. Valero, F. Bosché, Automatic Surface Flatness Control using Terrestrial Laser Scanning Data and the 2D Continuous Wavelet Transform, (2016) 2016.

[6] ASTM, Standard Test Method for Determining FF Floor Flatness and FL Floor Levelness Numbers (Metric 1, Astm. 96 (2015) 7–14. doi:10.1520/E1155M-96R08.2.

[7] M.J. Olsen, J.C. Allan, G.R. Priest, Movement and Erosion Quantification of the Johnson Creek, Oregon, Landslide through 3D Laser Scanning, in:

GeoCongress 2012: State of the Art and Practice in Geotechnical Engineering, 2012: pp. 3050–3059.
[8] B.A. Leshchinsky, M.J. Olsen, K. Hall, Enhancing Landslide Inventorying, Hazard Assessment and Asset Management Using Lidar, (2015).
[9] X. Xu, H. Yang, I. Neumann, Concrete crack measurement and analysis based on terrestrial laser scanning technology, Sens. Trans. J. 186 (2015) 168–172.
[10] M.J. Olsen, F. Kuester, B.J. Chang, T.C. Hutchinson, Terrestrial laser scanning-based structural damage assessment, Journal of Computing in Civil Engineering. 24 (2009) 264–272.
[11] Y. Turkan, S. Laflamme, L. Tan, Terrestrial Laser Scanning-Based Bridge Structural Condition Assessment, (2016).
[12] Y. Turkan, J. Hong, S. Laflamme, N. Puri, Adaptive wavelet neural network for terrestrial laser scanner-based crack detection, Automation in Construction. 94 (2018) 191–202. doi:10.1016/j.autcon.2018.06.017.
[13] A. Alhasan, D.J. White, K. De Brabanter, Wavelet Filter Design for Pavement Roughness Analysis, Computer-Aided Civil and Infrastructure Engineering. 31 (2016) 907–920. doi:10.1111/mice.12242.
[14] A. Alhasan, D.J. White, K. De Brabanterb, Automation in Construction Continuous wavelet analysis of pavement pro fi les, 63 (2016) 134–143. doi:10.1016/j.autcon.2015.12.013.
[15] A. Alhasan, D.J. White, K. De Brabanter, Spatial pavement roughness from stationary laser scanning, International Journal of Pavement Engineering. 18 (2017) 83–96. doi:10.1080/10298436.2015.1065403.
[16] P. Kumar, P. Lewis, C.P. Mcelhinney, A.A. Rahman, An algorithm for automated estimation of road roughness from mobile laser scanning data, Photogrammetric Record. 30 (2015) 30–45. doi:10.1111/phor.12090.
[17] A. Chin, M.J. Olsen, D. Ph, A.M. Asce, Evaluation of Technologies for Road Profile Capture, Analysis, and Evaluation, J. Surv. Eng. 141 (2015) 1–13. doi:10.1061/(ASCE)SU.1943-5428.0000134.
[18] E. Valero, F. Bosché, A. Forster, Automatic segmentation of 3D point clouds of rubble masonry walls, and its application to building surveying, repair and maintenance, Automation in Construction. 96 (2018) 29–39. doi:10.1016/j.autcon.2018.08.018.
[19] E. Valero, F. Bosché, A. Forster, L. Wilson, A. Leslie, Evaluation of historic masonry--Towards greater objectivity and efficiency, Heritage Building Information Modelling. Taylor & Francis. (2017).
[20] S. Fai, K. Graham, T. Duckworth, N. Wood, R. Attar, Building Information Modelling and Heritage Documentation, XXIII CIPA International Symposium, Prague, Czech Republic. (2011). doi: http://dx.doi.org/10.1136/adc.2010.183327.
[21] Y. Turkan, F. Bosche, C.T. Haas, R. Haas, Automated progress tracking using 4D schedule and 3D sensing technologies, Automation in Construction. 22 (2012) 414–421. doi:10.1016/j.autcon.2011.10.003.
[22] Y. Turkan, F. Bosche, C.T. Haas, R. Haas, Tracking Secondary and Temporary Concrete Construction Objects Using 3D Imaging Technologies, Computing in Civil Engineering. (2013) 749–756. doi:10.1017/CBO9781107415324.004.
[23] A. Braun, S. Tuttas, A. Borrmann, U. Stilla, Automated progress monitoring based on photogrammetric point clouds and precedence relationship graphs, Proceedings of the 32nd International Symposium on Automation and Robotics in Construction and Mining. (2015) 274–280.
[24] A. Braun, S. Tuttas, A. Borrmann, U. Stilla, A concept for automated construction progress monitoring using BIM-based geometric constraints and photogrammetric point clouds, Journal of Information Technology in Construction (ITcon). 20 (2015) 68–79.
[25] C. Kim, H. Son, C. Kim, Automated construction progress measurement using a 4D building information model and 3D data, Automation in Construction. 31 (2013) 75–82. doi:10.1016/j.autcon.2012.11.041.
[26] S. Kiziltas, Technological Assessment and Process Implications of Field Data Capture Technologies for Construction and Facility/Infrastructure Management, 13 (2008) 134–154.
[27] F. a Al-shalabi, Y. Turkan, a Novel Framework for BIM Enabled Facility Energy Management – a Concept Paper, (2015) 1–8.
[28] Roper, K., & Payant, The facility management handbook. (2014)
[29] B. Becerik-Gerber, F. Jazizadeh, N. Li, Application areas and data requirements for BIM-enabled facilities management, And Management. 138 (2011) 431–442. doi:10.1061/(ASCE)CO.1943-7862.0000433.
[30] P. Teicholz, BIM for Facility Managers, Wiley, Hoboken, NJ, 2013.
[31] L.Y. Liu, A.L. Stumpf, S.S. Kim, F.M. Zbinden, Capturing as-built project information for facility

management, in: Computing in Civil Engineering, 1994: pp. 614–621.
[32] M.-K. Kim, Q. Wang, J.-W. Park, J.C.P. Cheng, H. Sohn, C.C. Chang, Automated dimensional quality assurance of full-scale precast concrete elements using laser scanning and BIM, Automation in Construction. 72 (2016) 102–114. doi:10.1016/j.autcon.2016.08.035.
[33] F. Bosché, Automated recognition of 3D CAD model objects in laser scans and calculation of as-built dimensions for dimensional compliance control in construction, Advanced Engineering Informatics. 24 (2010) 107–118. doi:10.1016/j.aei.2009.08.006.
[34] M.K. Kim, J.C.P. Cheng, H. Sohn, C.C. Chang, A framework for dimensional and surface quality assessment of precast concrete elements using BIM and 3D laser scanning, Automation in Construction. 49 (2015) 225–238. doi:10.1016/j.autcon.2014.07.010.
[35] M.C. Israel, R.G. Pileggi, Use of 3D laser scanning for flatness and volumetric analysis of mortar in facades, 9 (2016) 91–106.
[36] P. Tang, B. Akinci, D. Huber, Characterization of three algorithms for detecting surface flatness defects from dense point clouds, IS&T/SPIE Electronic Imaging. 7239 (2009) 72390N–72390N. doi:10.1117/12.805727.
[37] F. Bosché, E. Guenet, Automating surface flatness control using terrestrial laser scanning and building information models, Automation in Construction. 44 (2014) 212–226. doi:10.1016/j.autcon.2014.03.028.
[38] M.J. Olsen, J.D. Raugust, G.V. Roe, Use of Advanced Geospatial Data, Tools, Technologies, and Information in Department of Transportation Projects, 2013. doi:10.17226/22539.
[39] R.A. Vincent, M. Ecker, others, Light detection and ranging (LiDAR) technology evaluation., 2010.